Revista Centro Azúcar
Vol. 52, 2025
ISSN: 2223-4861

Una Publicación de la Editorial Feijóo, UCLV

Disponible en:
http://centroazucar.uclv.edu.cu

http://scielo.sld.cu/scielo.php?script=sci_serial&pid=2223-4861&lng=es&nrm=iso

Artículo Original

ACCELERATED TEST TO DETERMINE THE CORROSION BEHAVIOR OF STEELS IN BOILERS BURNING SUGARCANE BIOMASS

ENSAYO ACELERADO PARA DETERMINAR EL COMPORTAMIENTO ANTE LA CORROSIÓN DE ACEROS EN CALDERAS QUE COMBUSTIONAN BIOMASA CAÑERA

Abel Rivas Gutierrez [1*] https://orcid.org/0009-0001-8807-5976
Carlos Lariot Sánchez [1] https://orcid.org/0000-0002-8727-3575
Beatriz Concepción Rosabal [1] https://orcid.org/0000-0003-1418-2186
Lizet Rodríguez Machín [2] https://orcid.org/0000-0001-8251-4440

[1] Instituto de Ciencia y Tecnología de Materiales (IMRE). Universidad de la Habana, La Habana, Cuba.
[2] Centro de Estudios Energéticos y Tecnologías Ambientales (CEETA). Facultad de Ingeniería Mecánica e Industrial. Universidad Central "Marta Abreu" de Las Villas, Santa Clara, Villa Clara, Cuba.

Recibido: Diciembre 2, 2024; Revisado: Diciembre 17, 2024; Aceptado: Diciembre 27, 2024

ABSTRACT

Introduction:
In order to increase the percentage of sugarcane agricultural residues used in a mixture with bagasse to generate electricity in biomass boilers, it is necessary to study the corrosion behavior caused in superheater tubes due to its high content of alkalis and chlorides compared to bagasse.

Objective:
To develop a tentative accelerated test, at laboratory scale, to predict the corrosion behavior, in high temperature zones, of type steels used in the superheater of high parameter steam generators.

Materials and Methods:
Metallography of steels, determination of composition and creation of synthetic ash to be used, corrosion rate calculation and analysis at the steel/oxides/deposits interface.

* Autor para la correspondencia: Abel Rivas, Email: abelrg1995@gmail.com

Results and Discussion:
In both steels studied, an increase in the corrosion rate was observed for the synthetic ash composition of the similar composition to that of higher concentration of sugarcane agriculture residues. Similarly, a greater thickness of oxide layers was observed when the steels were treated with synthetic ashes of composition similar to that of higher percentage of residues mixed with bagasse.
Conclusions:
This study carried out allowed to determine, comparatively, the behavior in the first stages of corrosion at 540 °C of two steels used in the construction of high-parameter superheaters boilers attacked by ashes simulating those formed in the combustion of different concentrations of sugarcane agricultural residues mixed with bagasse.

Keywords: ash; biomass; corrosion; steel; superheater.

RESUMEN

Introducción:
Para incrementar el porciento de residuos agrícolas cañeros que se utiliza en mezcla con bagazo, con el fin de generar energía eléctrica en calderas de biomasa, es necesario estudiar el comportamiento de la corrosión que causa en los tubos del sobrecalentador, debido a su alto contenido en álcalis y cloruros en comparación con el bagazo.
Objetivo:
Desarrollar un ensayo acelerado tentativo para pronosticar a escala de laboratorio el comportamiento, ante la corrosión en zonas de alta temperatura, de aceros tipo usados en el sobrecalentador de generadores de vapor de altos parámetros.
Materiales y Métodos:
Metalografía de aceros, determinación de composición y creación de ceniza sintética a utilizar, cálculo de velocidad de corrosión y análisis en la interfase acero/óxidos/depósitos.
Resultados y Discusión:
En ambos aceros estudiados se observó un incremento en la velocidad de corrosión para la composición de cenizas sintéticas de composición similar a la de mayor concentración de residuos de la agricultura de la caña. Igualmente, se observó un mayor grosor de las capas de óxidos al tratar los aceros con cenizas sintéticas de composición similar al de mayor porciento de residuos en mezcla con bagazo.
Conclusiones:
El estudio realizado permitió determinar, comparativamente, el comportamiento en las primeras etapas de la corrosión a 540 ºC de dos aceros empleados en la construcción de sobrecalentadores de calderas de altos parámetros atacados por cenizas que simularon las que se forman al combustionar diferentes concentraciones de residuos agrícolas cañeros en mezcla con bagazo.

Palabras clave: cenizas; biomasa; corrosión; acero; sobrecalentador.

1. INTRODUCTION

The need to replace the use of fossil fuels to renewable energy sources is clearly increasing worldwide. For island nations, this is not only an economic necessity due to high oil prices, but also because of its consequences on global warming, the most serious effects of which are rising sea levels and more intense weather events. However, the technology and resources necessary for a transition to renewable energy sources are not available to everyone.

Combustion is the most common method for generating electricity with biomass. This renewable and readily available resource makes a good candidate to solve this necessary and inevitable transition. In addition, biomass combustion has a greenhouse neutral effect because it releases the same amount of $CO_{2(g)}$ that the plant accumulates during its growth (Berlanga-Labari & Fernández-Carrasquilla, 2006). Corrosion can be caused by gaseous species in direct form, by deposits, or by a combination of both. In boilers, these problems are considered a significant drawback that can affect the design, lifetime, and operation of combustion equipment (Melissari, 2014). Inorganic composition of biomass causes serious deposition and corrosion problems, mainly in the superheater tubes due to be exposed to combustion gases (Muelas, 2016).

Cuba has a long tradition in the sugar agro-industry. Due to its high availability, sugarcane bagasse is a widely used biomass in the production of heat and electricity through cogeneration. The 2030 program to increase biomass electricity generation currently implemented by the country aims to exceed the 14 % of total electricity generation initially planned. To this goal, electricity should be generated from biomass approximately 300 days a year to achieve good financial indicators. In this program, the sugar industry plays an important role, but the bagasse produced during the harvest season is not enough for the intended 300 days of energy generation (Rubio-González et al., 2019). Sugarcane provides another type of biomass besides bagasse, known as sugarcane agricultural residues (RAC by its acronym in Spanish), constituted by tops and green and dried leafs. Although their use is not widespread worldwide, RAC are used as fuels in countries such as Cuba and Brazil (Rubio-González et al., 2021). Due to the uncertainty about the increased consequences of using RAC in high-parameter boilers, and also the recommendation of national specialists and boiler manufacturers, initially was approved to use RAC in quantities not exceeding 10 % mixed with bagasse. This amount only employs a portion of the available RAC, leaving a big part unutilized (Rubio-González et al., 2021).

The trend of many industrial processes and applications is to increase the temperature in service in order to obtain higher yields, but without reducing the service life of the components of the plant (Muelas, 2016).

Several studies (Rodríguez-Machín et al., 2018; Lariot-Sánchez et al., 2022) show that RAC has a higher content of ash than bagasse. This results in greater deposits on the boiler steels, affecting heat transfer and reducing the steam generation process efficiency, which leads to an increase in maintenance and cleaning downtime. Presence of alkalis in RAC is important in the corrosive processes in boiler metals. Even in small quantities, chemical elements such as chlorine or sulfur have high influence in the thermodynamic behavior of potassium during biomass combustion. In general, chlorine increase the potassium volatility in $KCl_{(g)}$ and $KOH_{(g)}$ gas phases. At superheaters

working temperature, potassium condenses as sulfide, chloride and silicate, forming deposits (Berlanga-Labari, & Fernández-Carrasquilla, 2006). Furthermore, a higher content of these compounds and elements has been reported in RAC than in bagasse.

The lower melting temperature of RAC ashes compared to bagasse makes them more aggressive, influencing incrustation and corrosion processes (Rubio-González et al., 2021). The most influential corrosion factors in superheater tubes are the tube surface temperature, the combustion gas temperature, the tube material and the chemical composition of deposits formed on the tubes. Several authors (Skrifvars et al., 2008; Skrifvars et al., 2010; O'Hagan et al., 2015; O'Hagan et al., 2016) demonstrate the possibility of determining, at the laboratory scale, the corrosion influence on steels at the superheater's operating temperature in contact with synthetic ashes simulating those from the biomass combustion. The research proposes a methodology to predict the high-temperature corrosion behavior of steel types used in superheater of high-parameter steam generators, based on comparative high-temperature test with synthetic ashes simulating those produced when burning, under the same conditions, bagasse-RAC mixtures.

The research's aim is to develop a tentative accelerated test to predict, on a laboratory scale, the high-temperature corrosion behavior of steel types used in the superheaters of high-parameter steam generators.

2. MATERIALS AND METHODS

A213T22 low alloy steel tubes (designated as T22) and A213TP321 stainless steel tubes (TP321) were employed. The tubes of 4.2 cm diameter were cut first into rings of 2.5 cm high, and later into 4 equal concave samples (coupons).

For the metallographic study of selected steels, the border flat surface of rings was polished to a specular shine, followed by chemical attack. NITAL-3 was used for T22, and a solution of $CuSO_4$ and HCl in distilled water, according to (ASTM E407-07, 2015), was used for TP321. After the attack, the samples were observed using a Nikon Eclipse MA200 optical microscope and a TESCAN VEGA 3 scanning electron microscope (SEM).

To confirm the chemical composition of these steels, they were analyzed by X-Ray Fluorescence spectrometry (XRF) using an Oxford Instruments X-Supreme energy dispersive X-ray spectrometer.

The synthetic salt used to simulate the chemical composition of ash produced by the bagasse-RAC biomass combustion, was prepared mixing the following pure analytical grade chemical reagents: $Fe_2(SO_4)_3$, $CaCl_2$, $MgCl_2$, KNO_3 and Na_3PO_4. The SiO_2 incorporated was obtained from rise husk ash, as shown in Table 1. To achieve its stoichiometric chemical composition based on its mass fraction and molarity, it was necessary to identified the quantities needs of these compounds to produce salts with a chemical composition similar to the ash produced by a bagasse-RAC mixture in 90-10 % currently used and 70-30 % ratio according to expected results. From now on this synthetic ash ratio will be defined as Bag-RAC ratio. These calculations considered the chemical composition of the biomass and ashes from bagasse and RAC reported by (Rubio-González et al., 2021).

Table 1. Starting compounds for the preparation of synthetic ash

Bag-RAC Ratio [wt. %]	*SiO_2**	*$Fe_2(SO_4)_3$*	*$CaCl_2$*	*$MgCl_2$*	*KNO_3*	*Na_3PO_4*
90-10	32.11	7.73	18.24	7.88	32.50	1.53
70-30	30.54	6.03	19.40	8.46	33.56	2.00

* Obtained from rice husk ash (Meneau-Hernández et al., 2021)

To obtain SiO_2 from rice husk, a byproduct of rice dehusking, the husk was first washed with tap water to remove soil residue. Subsequently, it was washed with dilute hydrochloric acid to remove metallic impurities (Fe, Ca, Mg, Na and K). Later it was vigorously stirred for 1 hour using an IKA RW 28 overhead stirrer; then the supernatant was separated, and the husk was washed with deionized water to remove excess of acid and chloride anions. The washed husk was dried at 100 °C in a Shanghai BOXUN oven and then calcined at 450 °C for 2 hours in a SX2-12TP muffle furnace to obtain the ash. This process ensures a SiO_2 purity of 92.7 wt. % (Meneau-Hernández et al., 2021).

To determine the corrosion rate by weight loss, a total of 20 steel coupons were tested: five samples per steel (T22 and TP321) and each simulated biomass ash mixture (90-10 % and 70-30 %). For the metallography and cross-sectional analysis, two samples per steel type and synthetic ash mixture were used, increasing the total number to 8 samples. Furthermore, because the samples would be subjected to elevated temperatures of 540 °C, two reference samples per steel type were added. This resulted in a total of 32 samples to be treated, 16 per each steel. The coupons dimensions were approximately 2.1 x 2.5 cm. They were mechanically cleaned to remove surface oxides, marked for subsequent identification, measured, and finally weighed. A paste was made by moistening the synthetic ash with deionized water. The paste was applied to the concave side of the coupons using a spatula (except for the reference samples). The coupons were treated in an industrial muffle at 540 °C for 72 hours, as shown in Figure 1.

Figure 1. Samples of steel with the synthetic ash mixture inside the muffle

The treated coupons for the corrosion rate determination were mechanically and chemically cleaned, then weighed for corrosion rate calculation according to (ASTM G1-03, 2017). Another set of samples was embedded in high-penetration resin (Araldite) to preserve the deposits and oxide layers formed after treatment for subsequent analysis. For this process, they were immersed in xylene for 30 minutes, then in xylene-Araldite 1:1 mixture for 3 hours, and finally in Araldite with accelerator and plasticizer placed under primary vacuum for 15 minutes to remove bubbles and

ensure high infiltration into the samples. Resin polymerization was carried out for 24 hours at 60 °C in an oven (Desmond, 1965).

The embedded samples, polished and coated with a 10 nm gold layer, were observed at a TESCAN VEGA 3 SEM to analyze in the micrographs the cross-section with an accelerating voltage of 10 kV for secondary electrons and 25 kV for backscattered electrons. The oxide layers thickness, formed between the steels and the deposits, was measured using the ImageJ software.

3. RESULTS AND DISCUSSION

Figure 2 shows superimposed XRF spectra of both steels, illustrating differences in Cr, Fe, Mn, and Ni concentrations.

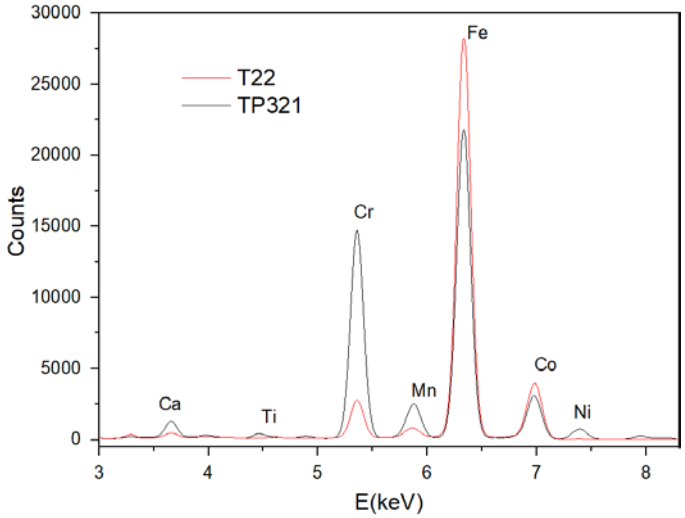

Figure 2. XRF spectra of T22 and TP321 steels

Table 2 shows the steels semi-quantitative analysis. These results are consistent with technical data sheet for the selected steels.

Table 2. Semi-quantitative analysis of chemical composition for selected steels

Steel	***Ni***	***Cr***	***Mo***	***Mn***	***Fe***	***Co***	***Cu***
T22	0.073	2.181	1.188	0.685	94.627	0.214	0.143
TP321	9.155	17.570	0.072	0.856	71.083	0.157	0.293

Optical micrograph of T22 (Figure 3a) shows ferrite phases (bright areas extending throughout the material) and sorbite (isolated darker areas) typical of this alloy. Electron micrograph of this steel (Figure 3c) shows interlaminar spaces of approximately 0.3 µm between the carbide lamellae, consistent with literature reports. In both the light and electron micrographs of TP321 (Figures 3b and 3d), martensitic laths derived from the original austenitic structure are observed.

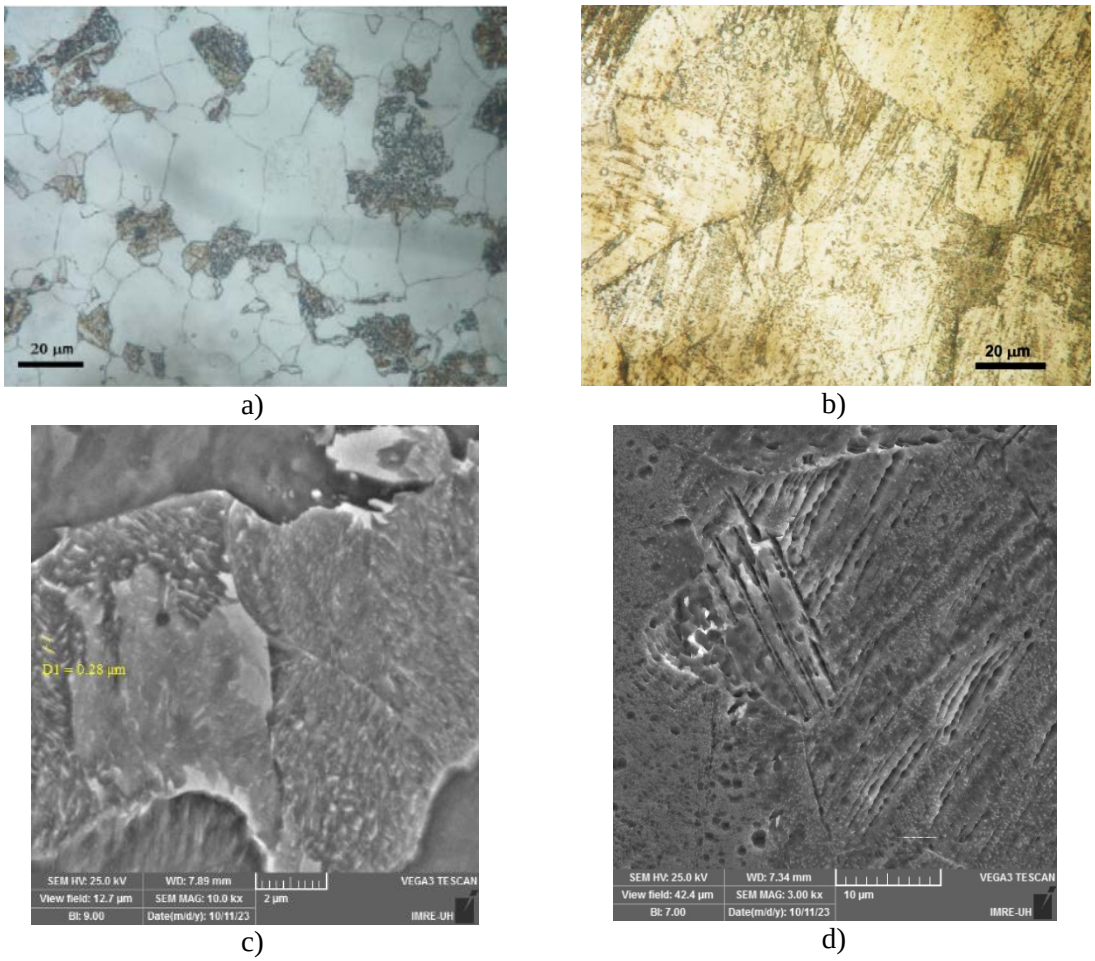

Figure 3. Optical and SEM micrographs show steels structures according to their type and chemical composition. Optical micrographs in (a) Ferrite-Sorbite in T22 steel, (b) Austenite-Martensite in TP321 steel and Secondary Electron SEM micrographs in (c) T22 steel and (d) TP321 steel

The treated coupons for corrosion rate determination were weighed after cleaning, and the corrosion rate was calculated (Table 3) according to (ASTM G1-03, 2017). The results show a higher corrosion rate in both steels with the highest proportion of the synthetic biomass ash mixture corresponding to RAC. As expected, a significant difference was observed between the corrosion rates of two steels, due to the TP321 is a stainless steel.

Table 3. Corrosion rate determined by weight loss method.

Steel	***Bag-RAC ratio [wt. %]***	***Weight loss [g]***	***Corrosion rate [g/(m²·h)]***
T22	90-10	0.42 ± 0.04	10.5 ± 0.9
T22	70-30	0.56 ± 0.06	11.9 ± 0.9
TP321	90-10	0.17 ± 0.02	3.8 ± 0.6
TP321	70-30	0.19 ± 0.03	4.5 ± 0.6

Cross-sectional SEM micrographs of steel/oxide/deposit interfaces are shown in Figures 4 and 5. Figure 4 shows a general overview of cross-section in secondary electron micrograph for enhanced topographical information. In this figure, are visible due to their brightness, areas corresponding to the resin (zone 2) around synthetic ash deposits

(zone 4) and also penetrating the space between steel (zone 1) and oxide layer (zone 3).

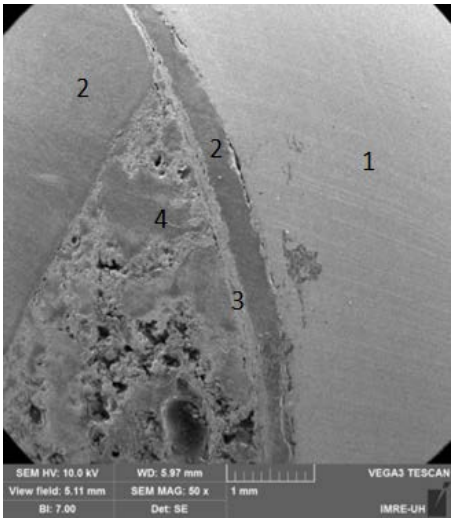

Figure 4. Secondary electron SEM micrograph of a cross-section of T22 steel treated at 540 °C with a rate of 90-10 Bagasse- RAC synthetic ash: 1) Steel, 2) Resin, 3) Oxide layer, 4) Synthetic ash deposits

The observations above were confirmed by backscattered electrons SEM micrographs (Figure 5), where the brightest areas correspond to the steel and oxide layers, and the darkest areas correspond to the resin and deposits. The SEM images showed poorly adherent oxide layers, with considerable separation observed between the steel and the oxide layers for all samples.

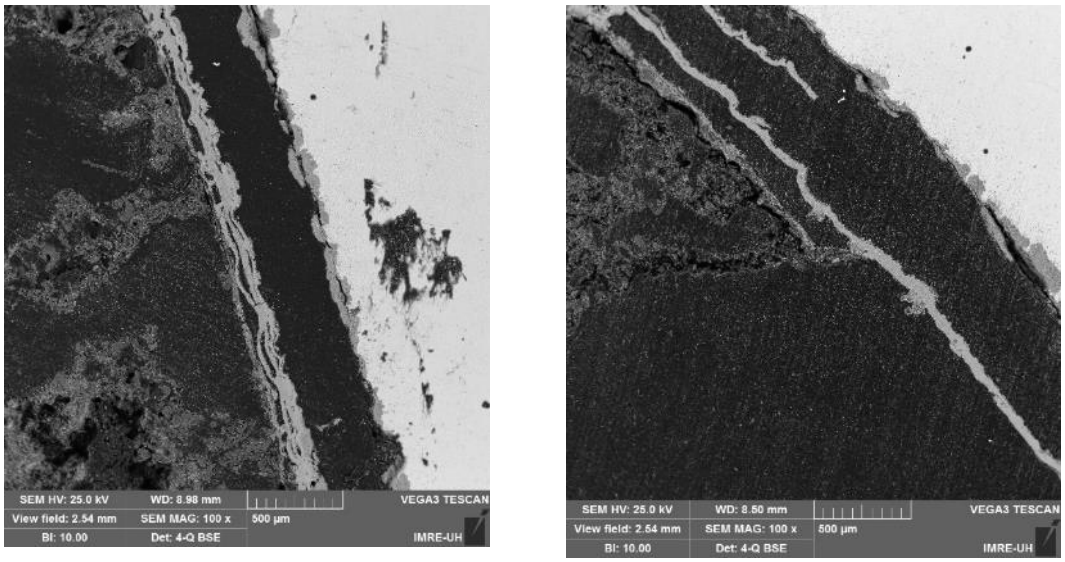

a) b)

Figure 5. Backscattered electron SEM micrographs of steel samples treated at 540 °C: a) T22 with synthetic ash rate 90-10 Bag-RAC; b) T22 with synthetic ash rate 70-30 Bag-RAC

The oxide layer thickness can be estimated from the images, showing greater thickness in samples treated with synthetic ashes containing a higher proportion of RAC (see Table 4). Furthermore, the TP321 steel samples exhibited thinner oxide layers compared to T22.

Table 4. Oxide layer thickness

Steel	*Bag-RAC ratio [wt. %]*	*Layer thickness [μm]*
T22	90-10	120-150
T22	70-30	135-170
TP321	90-10	70-105
TP321	70-30	80-120

During testing, corrosion progresses continuously due to the aggressiveness of the deposited ashes at high temperature. However, during sample cooling, stresses occur that detach the formed oxides from the metal. Nevertheless, thickness, oxide and deposit composition reflect how the process developed during the test.

4. CONCLUSIONS

This study comparatively validates the use of synthetic ashes to the determination of the initial corrosion behavior at 540 °C of two high-parameter boiler superheater steels exposed to ashes simulating those formed from combusting different concentrations of sugarcane agricultural residues mixture with bagasse. The corrosion test showed the tendency of both alloys to a higher corrosion rate with simulated ashes corresponding to the mixture with a higher percentage of RAC. This was also confirmed by SEM analysis of treated coupons that shows greater thickness of the formed oxide layers.

ACKNOWLEDGMENTS

The research that led to the results presented in this publication received funding from the International Funds and Projects Management Office under code PN 3602 LH 002-029. Acknowledge the IMRE, institution that provided sample preparation and SEM and XRF micrographs services. Thanks to CEINPET for providing access to the industrial muffle furnace. Finally, thanks to MINEM Power Plant Maintenance Center for donating the steels tested and conducting the optical metallography.

REFERENCES

ASTM E407-07., Standard Practice for Microetching Metals and Alloys, 2015. https://doi.org/10.1520/E0407-07R15E01

ASTM G1-03., Standard Practice for Preparing, Cleaning, and Evaluating Corrosion Test Specimens, 2017. https://doi.org/10.1520/G0001-03

Berlanga-Labari, C., & Fernández-Carrasquilla, J., Revisión sobre la corrosión de tubos sobrecalentadores en plantas de biomasa., Revista de Metalurgia, Vol. 42, No. 4, 2006, pp. 299-317. https://dialnet.unirioja.es/servlet/articulo?codigo=2143163

Desmond, K., Techniques for Electron Microscopy., Sir William Dunn School of Pathology, University of Oxford, Blackwell Scientific Publications, Second Edition, 1965, pp. 185-206.

Lariot-Sánchez, C., Rivas-Gutierrez, A., Rodríguez-Machín, L., Rubio-González, A., & Iturria-Quintero, P.J., Impact of Alkalis and Chlorides from Sugarcane Agriculture Residues on High Temperature Corrosion: A Review., Oxidation of Metals, Vol. 97, No. 5, 2022, pp. 451-475. https://doi.org/10.1007/s11085-022-10102-w

Melissari, B., Ash related problems with high alkali biomass and its mitigation-experimental evaluation., Memoria Investigaciones en Ingeniería, No. 12, 2014, pp. 31-44. https://dialnet.unirioja.es/servlet/articulo?codigo=4888804

Meneau-Hernández, R., Millán-Arrieta, J., Borrego-Morales, K., Alba-Carranza, M., & Farías-Piñeira, T., Adsorción de ciprofloxacina en materiales zeolíticos., Revista Cubana de Química, Vol. 33, No. 1, 2021, pp. 167-190. http://scielo.sld.cu/scielo.php?script=sci_arttext&pid=S2224-54212021000100167&lng=es&nrm=iso

Muelas, R., Recubrimientos resistentes a los fenómenos de degradación en las nuevas turbinas generadoras de energía por vapor de agua., Tesis presentada en opción al Grado Científico de Doctor en Ciencia y Tecnología de Materiales, Facultad de Ciencias Químicas, Universidad Complutense de Madrid, España, 2016. https://hdl.handle.net/20.500.14352/26917

O'Hagan, C.P., O'Brien, B.J., Griffin, F., Hooper, B., Leen, S.B., & Monaghan, R.F.D., Porosity-Based Corrosion Model for Alkali Halide Ash Deposits during Biomass Co-firing., Energy Fuels, Vol. 29, No. 5, 2015, pp. 3082-3095. https://pubs.acs.org/doi/10.1021/ef502275j

O'Hagan, C.P., O'Brien, B.J., Leen, S.B., & Monaghan, R.F.D., A microstructural investigation into the accelerated corrosion of P91 steel during biomass co-firing., Corrosion Science, Vol. 109, 2016, pp. 101-114. http://dx.doi.org/10.1016/j.corsci.2016.03.028

Rodríguez-Machín, L., Arteaga-Pérez, L.E., Pérez-Bermúdez, R.A., Casas-Ledón, Y., Prins, W., & Ronsse, F., Effect of citric acid leaching on the demineralization and thermal degradation behavior of sugarcane trash and bagasse., Biomass and Bioenergy, Vol. 108, 2018, pp. 371-380. https://doi.org/10.1016/j.biombioe.2017.11.001

Rubio-González, A.M., Galindo, P., Pérez, F.J., Ríos, P., Perdomo, L., Pérez, E., & Rubio, M.A., Estudio sobre el empleo de los residuos agrícolas cañeros como combustibles para la generación de electricidad en la industria azucarera cubana., Editorial Feijóo, Monografía, 2019, pp. 5-41. https://dspace.uclv.edu.cu/entities/publication/e75b0d49-47ed-4d2b-9661-e8335e9965d9

Rubio-González, A.M., Rodríguez-Machín, L., Iturria, P.J., Lariot, C.A., Rubio, M.A., Quiroga, D.A., Piloto, R., Duffus, A., Cabrera, L., Lorenzo, A., Brito, Á. L., Rivas, A., & García, Y., Estudio teórico conceptual sobre la corrosión en zonas de alta temperatura de generadores de vapor de altos parámetros. Editorial Feijóo, Monografía, 2021, pp. 10-101. http://feijoo.cdict.uclv.edu.cu/?monografia=estudio-teorico-conceptual-sobre-la-corrosion-en-zonas-de-alta-temperatura-de-generadores-de-vapor-de-altos-parametros

Skrifvars, B.J., Backman, R., Hupa, M., Salmenoja, K., & Vakkilainen, E., Corrosion of superheater steel materials under alkali salt deposits Part 1: The effect of salt deposit composition and temperature., Corrosion Science, Vol. 50, No. 5, 2008, pp. 1274-1282. https://doi.org/10.1016/j.corsci.2008.01.010

Skrifvars, B.J., Westén-Karlsson, M., Hupa, M., & Salmenoja, K., Corrosion of super-heater steel materials under alkali salt deposits. Part 2: SEM analyses of different

steel materials., Corrosion Science, Vol. 52, No. 3, 2010, pp. 1011–101. https://doi.org/10.1016/j.corsci.2009.11.026

CONFLICT OF INTEREST

The authors declare that there are no conflicts of interest.

AUTHORS' CONTRIBUTIONS

- BSc. Abel Rivas Gutierrez. Conceptualization, methodology, research, writing - first writing, software.
- Ph.D. Carlos Lariot Sánchez. Conceptualization, methodology, research, writing - review and editing.
- Ph.D. Beatriz Concepción Rosabal. Conceptualization, writing - review and editing, supervition.
- Ph.D. Lizet Rodríguez Machín. Project management, obtaining funding, writing - review and editing.